

Kinetic Properties of Intramembrane Charge Movement under Depolarized Conditions in Frog Skeletal Muscle Fibers

G. SZÜCS, Z. PAPP, L. CSERNOCH, and L. KOVÁCS

From the Department of Physiology, University Medical School, Debrecen, H-4012, Hungary

ABSTRACT Intramembrane charge movement was measured on skeletal muscle fibers of the frog in a single Vaseline-gap voltage clamp. Charge movements determined both under polarized conditions (holding potential, $V_H = -100$ mV; $Q_{\max} = 30.4 \pm 4.7$ nC/ μ F, $\bar{V} = -44.4$ mV, $k = 14.1$ mV; charge 1) and in depolarized states ($V_H = 0$ mV; $Q_{\max} = 50.0 \pm 6.7$ nC/ μ F, $\bar{V} = -109.1$ mV, $k = 26.6$ mV; charge 2) had properties as reported earlier. Linear capacitance (LC) of the polarized fibers was increased by $8.8 \pm 4.0\%$ compared with that of the depolarized fibers. Using control pulses measured under depolarized conditions to calculate charge 1, a minor change in the voltage dependence (to $\bar{V} = -44.6$ mV and $k = 14.5$ mV) and a small increase in the maximal charge (to $Q_{\max} = 31.4 \pm 5.5$ nC/ μ F) were observed. While in most cases charge 1 transients seemed to decay with a single exponential time course, charge 2 currents showed a characteristic biexponential behavior at membrane potentials between -90 and -180 mV. The voltage dependence of the rate constant of the slower component was fitted with a simple constant field diffusion model ($\alpha_m = 28.7$ s $^{-1}$, $\bar{V} = -124.0$ mV, and $k = 15.6$ mV). The midpoint voltage (\bar{V}) was similar to that obtained from the Q - V fit of charge 2, while the steepness factor (k) resembled that of charge 1. This slow component could also be isolated using a stepped OFF protocol; that is, by hyperpolarizing the membrane to -190 mV for 200 ms and then coming back to 0 mV in two steps. The faster component was identified as an ionic current insensitive to 20 mM Co^{2+} but blocked by large hyperpolarizing pulses. These findings are consistent with the model implying that charge 1 and the slower component of charge 2 interconvert when the holding potential is changed. They also explain the difference previously found when comparing the steepness factors of the voltage dependence of charge 1 and charge 2.

INTRODUCTION

The movement of intramembrane charges is believed to be the voltage-sensitive event that connects the surface and transverse tubular depolarization with the release of calcium from its intracellular store, the sarcoplasmic reticulum (SR), during contractile activation (Schneider and Chandler, 1973; Adrian and Almers, 1976a;

Address reprint requests to Dr. Géza Szücs, Department of Physiology, University Medical School, P. O. Box 22, Debrecen, H-4012, Hungary.

Chandler, Rakowski, and Schneider, 1976*a*). This hypothesis, based on the closely coupled voltage dependence of the two processes (Kovács, Rios, and Schneider, 1979; Rakowski, Best, and James-Kracke, 1985; Melzer, Schneider, Simon, and Szücs, 1986) was further strengthened by the description of the similar pharmacological sensitivity of the intramembrane charge movement and the contractile response (Huang, 1982; Hui, 1983; Berwe, Gottschalk, and Lüttgau, 1987; Caputo and Bolanos, 1987; Rios and Brum, 1987; Csernoch, Huang, Szücs, and Kovács, 1988).

Prolonged depolarization, which causes contractile refractoriness (Hodgkin and Horowicz, 1960), also results in the immobilization (or inactivation) of the charges that move in polarized fibers (Adrian, Chandler, and Rakowski, 1976; Chandler, Rakowski, and Schneider, 1976*b*; Rakowski, 1981). Moreover, a new type of charge movement seemed to appear in nonpolarized fibers moving in the hyperpolarizing direction and showing a mild voltage dependence (Adrian and Almers, 1976*b*; Adrian et al., 1976; Schneider and Chandler, 1976). This latter charge was named charge 2 to distinguish it from that of the polarized fibers (charge 1).

Brum and Rios (1987) suggested a close relationship between charge 1 and charge 2; namely, an interconversion upon changing the membrane potential, which means that the voltage sensor resides in its charge 1 position when the membrane is polarized and turns into charge 2 upon sustained depolarization. They also pointed out that some of the voltage sensors remain in the charge 2 state even in normally polarized fibers. These observations have recently been confirmed in the measurements of Caputo and Bolanos (1989) with the calcium antagonist D600. On the other hand, Brum and Rios (1987) and Caputo and Bolanos (1989) demonstrated that the maximal available charges measured as charge 1 and charge 2 were not identical and that there was a marked difference between the steepness values of the steady-state voltage dependences, too.

In this study we determined the charge movements in polarized and nonpolarized fibers using the single Vaseline-gap cut fiber technique of Kovács and Schneider (1978). The hyperpolarizing linear controls used conventionally for charge 1 determination contained considerably less charge 2 than in double or triple Vaseline-gap measurements (Brum and Rios, 1987; Caputo and Bolanos, 1989). Consequently, use of alternative controls at strong depolarizations made little material difference in the calculated amounts of charge 1. The data presented here are in accordance with the earlier reports mentioned above, indicating a considerably greater maximum amount and a more gradual voltage dependence of charge 2 as a whole than of charge 1. In contrast to these previous reports, the time course of our charge 2 transients fitted the sum of two exponentials indicating the movement of two kinetically different components, the faster of which had the characteristics of an outward anionic current. The slower component could be separated by returning in two steps to the holding potential after large hyperpolarizing pulses (stepped OFF protocol). The voltage dependence of the slower rate constant showed a midpoint voltage shifted in relation to that of charge 1, whereas its steepness factor resembled that of charge 1. These results are consistent with the interconversion model of Brum and Rios (1987), with the restriction that only the slower component of charge 2 is involved in the parallel shift that occurs in the voltage dependence of charge 1 and charge 2 when the holding potential is changed.

METHODS

Single muscle fibers were dissected from the m. semitendinosus of the frog (*Rana esculenta*) in Ringer's solution (115 mM NaCl, 2.5 mM KCl, 1.8 mM CaCl₂, 2 mM Tris-sodium-maleate buffer). Following relaxation after the K-contracture in a relaxing solution (120 mM K-glutamate, 2 mM MgCl₂, 0.1 mM EGTA, 5 mM Tris-sodium-maleate buffer), the fibers were cut ~5–8 mm from the tendon at the pelvic end and mounted in a single Vaseline-gap experimental chamber (Kovács and Schneider, 1978). After completing Vaseline isolation, the solution at the closed (tendon) end was changed to the external one (75 mM (TEA)₂SO₄, 10 mM Cs₂SO₄, 8 mM CaSO₄, 3 × 10⁻⁷ M tetrodotoxin, 5 mM Tris-sodium-maleate buffer), whereas the solution at the open end was changed to the internal one (105 mM Cs-glutamate, 5.5 mM MgCl₂, 0.1 mM EGTA, 0.0082 mM CaCl₂, 4.5 mM Tris-sodium-maleate buffer, 13.2 mM Tris-caesium-maleate buffer, 5 mM ATP, 5.6 mM glucose).

A voltage-clamp circuit was used to restore the membrane potential and control its changes. Currents accompanying depolarizing and hyperpolarizing pulses were recorded using an on-line connected microcomputer (HT-680X; HTSZ, Budapest, Hungary) and a 10-bit A/D converter, and the data were stored on a hard disk (SZM 5400; Izot, Sofia, Bulgaria). For further analysis an IBM PC/AT compatible computer (Varyter AT; MTA-SZTAKI-COSY, Budapest, Hungary) was used. All further details of dissection and data acquisition are given elsewhere (Kovács and Szücs, 1983; Csernoch, Kovács, and Szücs, 1987).

The measurements were carried out at low temperatures (4–6°C) by cooling the experimental chamber with Peltier devices.

Nonlinear capacitive currents representing intramembrane charge movement (Schneider and Chandler, 1973; Adrian and Almers, 1976a; Chandler et al., 1976a) were calculated from current transients measured on polarized (resting membrane potential, $V_H = -100$ mV) and nonpolarized ($V_H = 0$ mV) fibers. When fibers with normal resting membrane potentials were used, a method similar to the one described by Horowicz and Schneider (1981a) was applied. The current transients accompanying hyperpolarizing pulses of 30 mV and 100 ms (negative controls) were first baseline fitted (from 60 ms after the onset and offset of the pulse, respectively), then subtracted from the currents accompanying the depolarizing pulses. The nonlinear capacitive currents calculated in this way were then corrected for the sloping baseline to obtain the charge movement currents of the polarized fibers (charge 1).

Brum and Rios (1987) described a linear relationship between membrane potential and moving charge in nonpolarized fibers for pulses proceeding toward positive voltages. We have confirmed this observation in our measurements (data not shown), so currents charging the linear capacity were calculated from pulses polarizing the membrane to +30 or +60 mV for 100 ms (positive controls). Positive controls were then treated in the same way as negative controls and used to calculate the charge movement currents of the nonpolarized fibers (charge 2).

The steady-state voltage dependence ($Q(V)$) of charge 1 and charge 2 was fitted with the two-state Boltzmann distribution:

$$Q(V) = Q_{\max}/(1 + \exp(-\phi)) \quad (1)$$

In Eq. 1 $Q(V)$ is the amount of charge moved at voltage V , Q_{\max} is the maximal available charge, and ϕ is described by the equation

$$\phi = (V - \bar{V})/k \quad (2)$$

where \bar{V} is the voltage at which the charges are equally distributed between the two states and k is the steepness factor which includes the temperature and the effective valence of the moving charges.

To determine the kinetic properties of the charge transfer, an exponential function was fitted to the current transients starting 8 ms after the onset and offset of the pulse. The 8 ms point was chosen to allow for transverse-tubular delays (Adrian and Peachy, 1973; Simon and Beam, 1985). In the case of charge 1, a secondary slow component ("hump") appears on the charge movement currents at certain voltages (Horowicz and Schneider, 1981*b*; Huang, 1981). The currents at which these "humps" were clearly visible were left out from further analysis. When fitting charge movement currents of nonpolarized fibers (that is, charge 2), a single exponential did not describe the falling phase properly at every voltage (see Results). When fitting those currents, a sum of two exponentials was used.

To describe the voltage dependence of the rate constant ($\alpha(V)$) of the charge transfer, the constant field diffusion model was used (Chandler et al., 1976*a*; Benz and Zimmermann, 1983):

$$\alpha(V) = \frac{\phi}{2} \alpha_m \operatorname{cth}(\phi/2) \quad (3)$$

where α_m is the rate constant at voltage \bar{V} , and ϕ and \bar{V} have their usual meanings (see Eq. 2).

When fitting Eq. 1 or 3 to the experimental data, the linear least-squares method was used (see, for example, Scarborough, 1966). Averages are expressed as mean \pm SD.

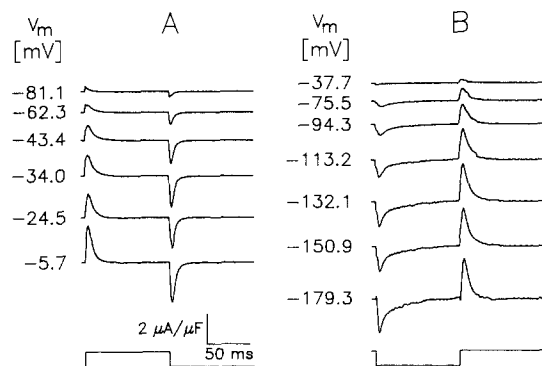


FIGURE 1. Charge movement currents recorded under (A) polarized ($V_H = -100$ mV) and (B) depolarized ($V_H = 0$ mV) conditions. The fiber was depolarized or hyperpolarized for 100 ms to the voltage indicated next to the traces. To calculate the linear capacity (LC) in the polarized state, the "negative control" (LC = 7.94 μ F) was used, while in the depolarized state the "positive control"

(LC = 7.07 μ F) was used. The sloping baseline was fitted to a 30-ms-long section starting 70 ms after the onset of the potential change for both the ON and the OFF parts. Fiber 71209; fiber diameter (d) = 89 μ m, sarcomere length (s) = 2.3 μ m, temperature (T) = 3.7°C.

RESULTS

Steady-State Distribution of Charge 1 and Charge 2

To compare our results to previous measurements, we determined the voltage dependence of charge 1 and charge 2 in the single Vaseline gap using generally accepted methods. In the experiment shown in Fig. 1, the membrane was first voltage-clamped to 0 mV and then hyperpolarizing (test) pulses with increasing amplitude were applied. Two positive controls (pulses to +30 or +60 mV; see Methods) bracketed each of the two test pulses. All recorded controls were averaged to obtain the mean positive control that was used for further analysis. The calculated charge movement currents are shown in Fig. 1 B. When completing the recordings

on the depolarized fiber, the membrane potential was changed to -100 mV and depolarizing (test) pulses were applied. The mean negative control used to calculate the charge movement currents (Fig. 1A) was averaged from all negative controls (pulses to -130 mV). In several cases we were able to measure charge 2 again after changing the membrane potential back to 0 mV. There was no significant difference between the two runs either in the amount or in the voltage dependence of movable charges.

To determine the steady-state voltage dependence, Eq. 1 was fitted to the experimental data. In the case of the fiber shown in Fig. 1, the best-fit parameters are $Q_{\max} = 35.4$ and 48.9 nC/ μ F, $\bar{V} = -32.2$ and -104.7 mV, and $k = 19.9$ and 24.7 mV for charge 1 and charge 2, respectively. Experiments carried out in the same way

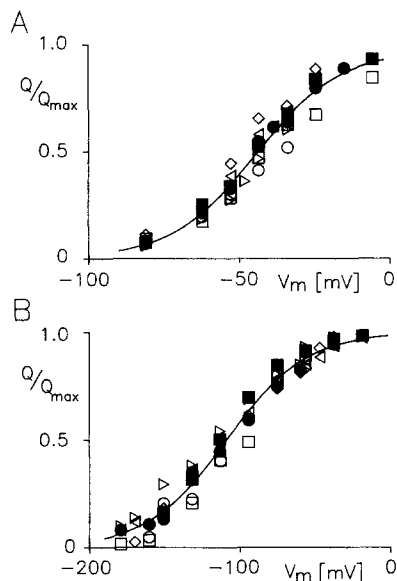


FIGURE 2. Steady-state membrane potential dependence of normalized charges in polarized (A) and depolarized (B) fibers. The data were normalized to the maximal available charge on the given fiber and in the given polarization state. The continuous curves were then generated by fitting Eq. 1 to all data points. Best-fit parameters are $\bar{V} = -44.4$ and -109.1 mV and $k = 14.1$ and 26.6 mV for the polarized and depolarized states, respectively. Separate fits of Eq. 1 to the data of each individual fiber ($n = 7$) resulted in an average maximal mobile charge of 30.4 ± 4.7 and 50.0 ± 6.7 nC/ μ F (normalized to the linear capacitance) for charge 1 and charge 2, respectively. Fibers 71116 (■), 71125 (●), 71126 (◁), 71201 (◇), 71202 (▷), 71208 (□), and 71209 (○); $d = 82$ – 104 μ m, $s = 2.1$ – 2.4 μ m, $T = 3.7$ – 5.1 °C.

resulted in an averaged maximal charge of 30.4 ± 4.7 and 50.0 ± 6.7 nC/ μ F on polarized and depolarized fibers ($n = 7$).

To obtain an overall voltage dependence, all values were normalized to the maximal available charge of the corresponding fiber and polarization state. The normalized values are shown in Fig. 2 for polarized (A) and depolarized (B) conditions. All the normalized data points were fitted with the two-state Boltzmann function (Eq. 1). The parameters of these fits are $\bar{V} = -44.4$ and -109.1 mV and $k = 14.1$ and 26.6 mV for charge 1 and charge 2, respectively. The values obtained are generally in good agreement with the previous results (Brum and Rios, 1987; Caputo and Bolanos, 1989), except that the amount of charge 2 seems to be bigger than was reported in those communications.

Charge 1 Calculated with Positive Controls

The work of Brum and Rios (1987) showed the existence of charge 2 in polarized fibers and raised the possibility of an error in charge 1 calculations resulting from the nonlinearity of the negative controls. In 12 fibers we compared the linear capacitance data (Table I) calculated from positive (A) and negative controls (B) taken just before and after polarization. The values clearly indicate an additional capacitance present in the negative controls of polarized fibers with an average increase of $8.8 \pm 4.0\%$ (Table I, column C).

This additional capacitance arises from a nonlinear charge movement, presumably charge 2, present in the negative controls. Using the positive controls measured in the depolarized state to calculate this nonlinear charge movement, an average value

TABLE I
Nonlinear Charge Movement in the Negative Control

Fiber	Linear capacitance		B/A	Q
	$V_H = 0$ mV	$V_H = -100$ mV		
	μF			
71116	15.77	17.10	1.084	1.54
71118	10.14	11.23	1.107	2.82
71123	10.26	11.70	1.140	3.32
71125	16.03	18.41	1.148	3.01
71126	14.46	14.75	1.020	0.30
71201	8.96	9.66	1.078	1.45
71202	26.66	27.70	1.039	1.03
71208	11.25	12.25	1.089	1.83
71209	7.07	7.94	1.123	2.60
80106	22.52	23.25	1.032	1.12
80107	8.95	10.00	1.117	2.43
80126	11.71	12.55	1.072	1.15
Mean	13.65	14.71	1.088	1.88
\pm SD	5.62	5.68	0.040	0.90

of 1.88 ± 0.90 nC/ μF was found. To determine the total amount of charge 2 present under polarized conditions, hyperpolarizing pulses to -170 mV were applied and an average value of 5.6 ± 2.5 nC/ μF was found ($n = 7$). These values are considerably lower than those reported by Brum and Rios (1987) for the double Vaseline gap. On the other hand, they suggest that calculations of charge 1 under single Vaseline-gap conditions are not contaminated with large errors when linear capacity is determined using the negative controls. To test this directly, we also calculated charge 1 with positive controls on the same fibers. Through an approach similar to that described above, the average maximal charge determined in this way increased (to 31.4 ± 5.5 nC/ μF), whereas the overall voltage dependence was only slightly modified ($\bar{V} = -44.6$ mV, $k = 14.5$ mV).

The above data indicate that charge 2 also shows a larger maximum value and a less steep voltage dependence than charge 1 in single Vaseline-gap voltage clamp, independent of the choice of control pulse protocols for calculating charge 1. Such a finding would need to be reconciled to the hypothesis that charge 1 and charge 2 result from the same charge entity by interconverting with shifts in the holding potential (Brum and Rios, 1987). The change in the slope (parameter k in Eq. 2) of the voltage dependence, for example, would mean a change in the effective valence of the charged molecule. That is, either the moving charge itself or the membrane thickness across which it can move has changed. Since the change is almost twofold (from 14.1 to 26.6 mV), it would mean a drastic alteration in the molecule responsible for charge movement. To explore such a modification, we determined the steepness factor (k) in an alternative way, namely, from the kinetics of charge movement.

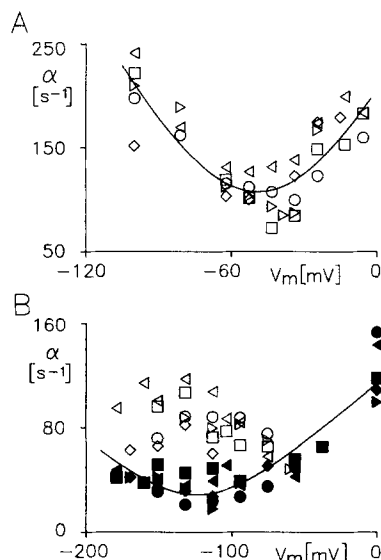


FIGURE 3. Voltage dependence of the rate constants of charge 1 (A) and charge 2 (B). Single exponentials were fitted to the ON and OFF transients starting 8 ms after the onset of the membrane potential change. In the case of the charge 2 currents, at membrane potentials of -90 mV and more negative, two exponentials (indicated by filled and open symbols) were necessary to describe the kinetics of the charge transfer. Two of the seven fibers in Fig. 2 showed distinct "hump" components on the charge 1 records and were left out of the kinetic analysis. The continuous curves show the best fits of Eq. 3 to the rate constants of charge 1 (with $\alpha_m = 107.5$ s^{-1} , $\bar{V} = -49.2$ mV, and $k = 13.5$ mV) and to that of the slow

component of charge 2 (with $\alpha_m = 28.7$ s^{-1} , $\bar{V} = -124.0$ mV, and $k = 15.6$ mV). Fibers 71209 (\triangleleft), 71208 (\square), 71126 (\triangleright), 71125 (\diamond), and 71116 (\circ).

Voltage Dependence of the Rate Constants

A single exponential was fitted to the charge movement currents as described in the Methods to characterize the kinetic behavior of the charge transfer. The rate constants obtained are plotted vs. voltage in Fig. 3. In two of the seven fibers used for studying steady-state charge vs. voltage distribution, the secondary "hump" component was so pronounced on the charge 1 records that fitting was impossible in a ~ 20 -mV range (from -55 to -35 mV). These fibers were left out of further analysis.

Under depolarized conditions at -90 mV, and at more negative voltages, two kinetically different components were present in the charge movement currents (see,

for example, the trace at -150.9 mV in Fig. 1). In these cases the sum of two exponentials was used for the fit and the rate constants of both the slower and the faster components are shown in Fig. 3 B.

Despite the scatter in the data at and around -50 mV (probably due to the "hump" component present), a reasonable fit of Eq. 3 was achieved for charge 1. The parameters ($\alpha_m = 107.5$ s $^{-1}$, $\bar{V} = -49.2$ mV, and $k = 13.5$ mV) are not only close to those reported earlier, but agree well with those of the steady-state charge vs. voltage distribution. In depolarized fibers only the slower rate constants (filled symbols in Fig. 3 B) showed the characteristic bell-shaped voltage dependence, and they were fitted with Eq. 3 (the best-fit parameters being $\alpha_m = 28.7$ s $^{-1}$, $\bar{V} = -124.0$ mV, and $k = 15.6$ mV). While α_m and \bar{V} were found to be close to the previous reports (Brum and Rios, 1987), the steepness (k) resembled the value obtained for charge 1 rather than that of the charge vs. voltage distribution of charge 2.

This finding gave rise to the assumption that only the slow component of charge 2 corresponds to the voltage sensor of excitation-contraction coupling, while the fast component is of different origin. To test this hypothesis further, measurements to separate the two components were designed.

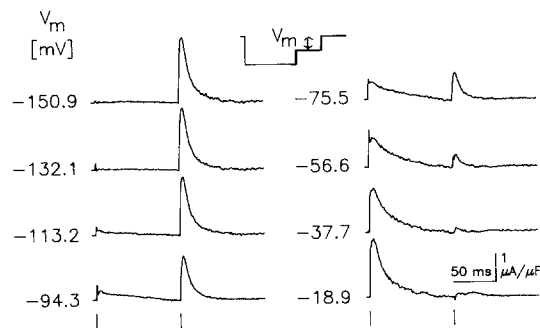


FIGURE 4. Charge movement currents recorded with the stepped OFF protocol. The membrane was hyperpolarized to -190 mV for 200 ms and then depolarized back to 0 mV in two steps (see inset; the thick line shows the sampled period). The vertical bars below the traces mark the start of the first and second OFF steps, while the numbers next to each trace

indicate the membrane potential during the first OFF step. Fiber 80126; $d = 106$ μm , $s = 2.7$ μm , $T = 4.9^\circ\text{C}$.

Stepped OFF Protocol to Isolate the Slow Component of Charge 2

Brum and Rios (1987) reported significant ON and OFF inequality of charge 2 which disappeared when large hyperpolarizing (conditioning) pulses or calcium-free external solutions were applied. They interpreted these findings as resulting from a calcium conductance being present in depolarized fibers and decreasing on hyperpolarizing pulses.

On the basis of these data we studied the charge movements on depolarized fibers by stepping first to a large hyperpolarized membrane potential and then coming back, with a depolarizing pulse, to the desired test potential. Fig. 4 shows charge movement currents recorded with this strategy. The membrane was hyperpolarized to -190 mV for 200 ms, then depolarized first to the test pulse level for 100 ms, and finally back to the holding potential (stepped OFF protocol; see Fig. 4, *inset*).

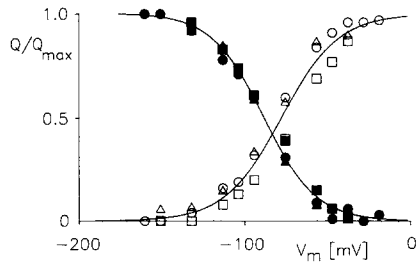


FIGURE 5. Membrane potential dependence of normalized charge for the first (*open symbols*) and second (*filled symbols*) OFF steps during the stepped OFF protocol. The values were normalized to the maximal charge determined on the corresponding fiber. The average value of this maximal charge was found to be 33.9 ± 5.9 nC/ μ F ($n = 3$). The continuous lines are the best fits of Eq. 1 to all data points with $\bar{V} = -78.0$ and -88.4 mV and $k = 17.1$ and 15.8 mV for the first and second steps, respectively. Fibers 71208 (\square), 71209 (\circ), and 80126 (\triangle); $d = 89$ – 106 μ m, $s = 2.1$ – 2.7 μ m, $T = 3.7$ – 4.9° C.

continuous lines are the best fits of Eq. 1 to all data points with $\bar{V} = -78.0$ and -88.4 mV and $k = 17.1$ and 15.8 mV for the first and second steps, respectively. Fibers 71208 (\square), 71209 (\circ), and 80126 (\triangle); $d = 89$ – 106 μ m, $s = 2.1$ – 2.7 μ m, $T = 3.7$ – 4.9° C.

The amount of charges moved during the first OFF step increases toward more depolarized membrane potentials, as expected, but the kinetics of this charge transfer seems to be described by a single exponential function, in contrast to the charge 2 currents accompanying simple hyperpolarizing pulses. Fig. 5 plots the normalized charge vs. voltage distribution for the first (*open symbols*) and second (*filled symbols*) OFF steps (three fibers). The second step moves less and less charge as the first moves more and more. The solid curves are the best fits of Eq. 1 to the data with the parameters of $\bar{V} = -78.0$ and -88.4 mV and $k = 17.1$ and 15.8 mV for the first and second steps, respectively. The average maximal charge determined from the individual fits was 33.9 ± 5.9 nC/ μ F. On the grounds of the similarity between the values obtained for parameter k , the stepped OFF protocol was used to isolate the slow component of charge 2.

Fig. 6 shows a detailed kinetic analysis of the charge movement currents on a fiber where, besides the charge 1 measurements (*diamonds*), both the simple (*circles*) and the stepped OFF charge 2 protocols (*squares*) were completed. On this fiber the

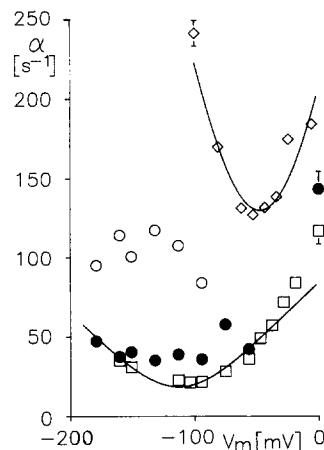


FIGURE 6. The voltage dependence of the kinetics of charge 1 (\diamond) and charge 2 measured with hyperpolarizing steps (\circ , \bullet) or with the stepped OFF protocol (\square). For charge 2 determined in the conventional way, both the slower (\bullet) and the faster (\circ) components are shown. The value (with the error bar) at -100 mV (charge 1) and at 0 mV (charge 2) is the average (\pm SD) rate constant determined from the OFF currents or the second OFF step (stepped OFF protocol). The solid lines represent the best fits of Eq. 3 to the data of charge 1 ($\alpha_m = 129.8$ s $^{-1}$, $\bar{V} = -47.5$ mV, $k = 16.7$ mV) and to the data of the stepped OFF protocol ($\alpha_m = 18.6$ s $^{-1}$, $\bar{V} = -113.0$ mV, $k = 12.5$ mV). Same fiber as in Fig. 1.

mV, $k = 16.7$ mV) and to the data of the stepped OFF protocol ($\alpha_m = 18.6$ s $^{-1}$, $\bar{V} = -113.0$ mV, $k = 12.5$ mV). Same fiber as in Fig. 1.

stepped OFF protocol clearly eliminated the fast component of charge 2. Charge 1 currents, as usual, were much faster than those of charge 2 at every voltage examined.

The solid lines in Fig. 6 represent the best fits of Eq. 3 to the rate constants of the stepped OFF protocol and to those of the charge 1 currents; the parameters of the fit are $\alpha_m = 129.8$ and 18.6 s^{-1} , $\bar{V} = -47.5$ and -113.0 mV , and $k = 16.7$ and 12.5 mV , respectively. Though there is a considerable difference both in the voltage dependence and in the speed of the charge transfer, the effective valence is, within experimental error, preserved.

Is the Fast Component of Charge 2 a Calcium Current?

In contrast to the finding of Brum and Rios (1987), we have not observed ON and OFF inequality when measuring charge 2 using simple hyperpolarizing pulses. The data from the stepped OFF protocol, however, seemed to favor the interpretation that the fast component of charge 2 results from a calcium current. To test this possibility directly, 20 mM Co^{2+} was used in the external solution to block calcium conductance, if present. Fig. 7 shows the rate constants of charge 2 in the reference

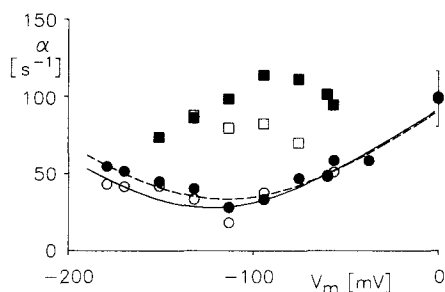


FIGURE 7. Effect of 20 mM Co^{2+} on the kinetics of charge 2. Both the slower (circles) and faster (squares) components of charge 2 were observed before (open symbols) and after (filled symbols) the addition of the cobalt. The curves are the best fit of Eq. 3 to the data in control solution (solid line; $\alpha_m = 27.9 \text{ s}^{-1}$, $\bar{V} = -112.6 \text{ mV}$, $k = 18.7 \text{ mV}$) and in the presence of 20 mM Co^{2+} (dashed line; $\alpha_m = 33.5 \text{ s}^{-1}$, $\bar{V} = -115.0 \text{ mV}$, $k = 21.5 \text{ mV}$). Fiber 71126; $d = 96 \text{ }\mu\text{m}$, $s = 2.1 \text{ }\mu\text{m}$, $T = 4.6^\circ\text{C}$.

solution (open symbols) and in the presence of 20 mM Co^{2+} (filled symbols). The lines represent the best fits of Eq. 3 to the slow component of charge 2 (circles). These data clearly indicate that the cobalt exerted no significant effect on either the slow or the fast component of charge 2. If anything, the latter is even more pronounced.

DISCUSSION

Charge 2 in Negative Controls

There are contradictory data concerning the presence of charge 2 under polarized conditions using intact fibers (Adrian et al., 1976; Adrian and Almers, 1976a; Schneider and Chandler, 1976) or the single Vaseline-gap technique (Horowicz and Schneider, 1981a) and double (Brum and Rios, 1987) or triple Vaseline gaps (Caputo

and Bolanos, 1989). The latter works showed a considerable amount of charge 2 present in fibers with normal membrane potentials and suggested the use of alternative controls taken either on depolarized fibers (Brum and Rios, 1987) or at hyperpolarized potentials (Caputo and Bolanos, 1989).

In our single Vaseline-gap experiments, hyperpolarizing controls taken from polarized fibers contained much less nonlinear charge than in the earlier reports. Consequently, the calculated amount of charge 1 depended only to a small extent on the control used. This finding explains why earlier reports (e.g., Horowicz and Schneider, 1981a) overlooked this phenomenon. Although a clear explanation is missing, the experimental conditions, especially stretching, might be responsible for this difference.

An approximation of the total charge in polarized fibers under our conditions would be the sum of the maximal charge determined as charge 1 with positive controls (31.4 nC/ μ F) and the charge moving in the hyperpolarizing direction (5.6 nC/ μ F, measured with pulses to -170 mV and calculated with positive controls). Though this results in a 37.0 nC/ μ F total charge, which is, on the one hand, closer to that measured for charge 2 (50.0 ± 6.7 nC/ μ F) and, on the other hand, similar to the values reported by Brum and Rios (1987) and Caputo and Bolanos (1989), there still exists a difference in movable charges under polarized and nonpolarized conditions.

Alternative Ways to Fit the Voltage Dependence of the Rate Constant

The conclusion that the steepness factor of the slow component of charge 2 resembles that of charge 1 might be a consequence of choosing the constant field theory to describe the voltage dependence of the rate constants. To apply a physically more realistic approach, we also fitted the rate constants using a second-order, one-barrier Eyring rate model similar to that used by Simon and Beam (1985) and Brum and Rios (1987). The model assumes that the transition between the resting and activated states of the charge depends exponentially on the free energy difference of the two states (Tsien and Noble, 1969), and this free energy is a second order polynomial function of the membrane voltage.

The above model leads to the equation

$$\alpha(V) = \frac{1}{2}\alpha_m \exp(a\phi^2/4) \cosh(\phi/2) \quad (4)$$

where a is a constant expressing the dependence on the second power of the membrane potential, while α_m and ϕ have their usual meanings. The best-fit parameters of Eq. 4 to the data in Fig. 3 are $\alpha_m = 106.3$ and 21.2 s $^{-1}$, $a = 0.12$ and 0.14 , $\bar{V} = -48.9$ and -117.9 mV, and $k = 14.2$ and 17.2 mV for charge 1 and charge 2, respectively. These data indicate that the similarity between the steepness factors also exists when they are calculated on the basis of the Eyring model.

Using the Stepped OFF Protocol for Charge 2 Measurements

The stepped OFF protocol proved to be a useful tool for separating charge movement components on depolarized fibers. There are, however, two problems with this approach. First, the maximal amount of charge determined in this way (33.9 nC/ μ F) is less than its total amount on polarized fibers (37.0 nC/ μ F, as calculated

previously). Second, the midpoint voltages (\bar{V}) determined from the Q vs. V and α vs. V plots differ by ~ 25 mV, the latter being less negative.

The first problem seems to be only a virtual one. It follows from the steady-state distribution of charge 2 (Fig. 2 *B*) that not all the charges are moved by a pulse to -190 mV. The remaining charges (2.3 nC/ μ F) explain, within experimental error, the difference mentioned above, supposing that all or most of this remaining charge population is part of the slow component. We have no explanation for the second problem. It probably originates from errors present in both the charge and the rate constant data.

An Anionic Current Present on Depolarized Fibers

Another possible origin of the fast component might be an outward current carried by anions, presumably by Cl^- . Single channel experiments (Blatz and Magleby, 1983; Woll, Leibowitz, Neumke, and Hille, 1987) indicated the presence of chloride-selective channels with large conductances in depolarized skeletal muscle fibers. These channels showed inactivation on hyperpolarizing voltage steps. To test the possible role of a Cl^- current, the effect of anthracene-9-carboxylic acid (5 mM), a chloride channel blocker (Palade and Barchi, 1977), was investigated and reductions in the fast component were observed (data not shown). This component is therefore probably a chloride current.

Other data, however, render this interpretation less convincing. Anthracene was found to be a twitch potentiator on polarized fibers, which shifted the voltage dependence of charge 1 toward negative membrane potentials (a ~ 15 -mV shift occurs when applying 5 mM anthracene; unpublished observations). The underlying mechanism is possibly a surface charge effect (Palade and Barchi, 1977), which would be present on depolarized fibers as well. Furthermore, anthracene, though in lower concentrations (10^{-5} – 10^{-4} M) than those used here, has been shown to be a less potent blocker of amphibian than of mammalian chloride channels (Bryant and Morales-Aguilera, 1971; Woll et al., 1987).

The results presented here demonstrate the presence of kinetically different charge 2 components in depolarized fibers. Both components seem to be conserved, but only the slower interconverts with charge 1. This slower component may reflect the movement of the voltage sensor of excitation–contraction coupling in its inactivated state, whereas the faster is presumably a chloride current.

This work was supported by a Hungarian research grant (OTKA 119) and by the Muscular Dystrophy Association.

Original version received 26 June 1990 and accepted version received 6 February 1991.

REFERENCES

- Adrian, R. H., and W. Almers. 1976a. The voltage dependence of membrane capacity. *Journal of Physiology*. 254:317–338.
- Adrian, R. H., and W. Almers. 1976b. Charge movement in the membrane of striated muscle. *Journal of Physiology*. 254:339–360.
- Adrian, R. H., W. K. Chandler, and R. F. Rakowski. 1976. Charge movement and mechanical repriming in striated muscle. *Journal of Physiology*. 254:361–388.

- Adrian, R. H., and L. D. Peachey. 1973. Reconstruction of the action potential of frog sartorius muscle. *Journal of Physiology*. 235:103–131.
- Benz, R., and U. Zimmerman. 1983. Evidence for the presence of mobile charges in the cell membrane of *Valonia utricularis*. *Biophysical Journal*. 43:13–26.
- Berwe, D., G. Gottschalk, and H. C. Lüttgau. 1987. Effects of the calcium antagonist Gallopamil (D600) upon excitation-contraction coupling in toe muscle fibers of the frog. *Journal of Physiology*. 385:693–707.
- Blatz, A. L., and K. L. Magleby. 1983. Single voltage-dependent chloride-selective channels of large conductance in cultured rat muscle. *Biophysical Journal*. 43:237–241.
- Brum, G., and E. Rios. 1987. Intramembrane charge in frog skeletal muscle fibres: properties of charge 2. *Journal of Physiology*. 387:489–517.
- Bryant, S. H., and A. Morales-Aguilera. 1971. Chloride conductance in normal and myotonic muscle fibres and the action of mono-carboxylic acids. *Journal of Physiology*. 219:367–383.
- Caputo, C., and P. Bolanos. 1987. Contractile inactivation in frog skeletal muscle fibers. The effect of low calcium, tetracaine, dantrolene, D-600, and nifedipine. *Journal of General Physiology*. 94:421–442.
- Caputo, C., and P. Bolanos. 1989. Effects of D-600 on intramembrane charge movement of polarized and depolarized frog muscle fibers. *Journal of General Physiology*. 94:43–64.
- Chandler, W. K., R. F. Rakowski, and M. F. Schneider. 1976a. A non-linear voltage dependent charge movement in frog skeletal muscle. *Journal of Physiology*. 254:245–283.
- Chandler, W. K., R. F. Rakowski, and M. F. Schneider. 1976b. Effects of glycerol treatment and maintained depolarization on charge movement in muscle. *Journal of Physiology*. 254:285–316.
- Csernoch, L., C. L.-H. Huang, G. Szücs, and L. Kovács. 1988. Differential effects of tetracaine on charge movements and Ca^{2+} signals in frog skeletal muscle. *Journal of General Physiology*. 92:601–612.
- Csernoch, L., L. Kovács, and G. Szücs. 1987. Perchlorate and the relationship between charge movement and contractile activation in frog skeletal muscle fibres. *Journal of Physiology*. 390:213–227.
- Hodgkin, A. L., and P. Horowicz. 1960. Potassium contractures in single muscle fibres. *Journal of Physiology*. 153:386–403.
- Horowicz, P., and M. F. Schneider. 1981a. Membrane charge movement in contracting and non-contracting skeletal muscle fibres. *Journal of Physiology*. 314:565–593.
- Horowicz, P., and M. F. Schneider. 1981b. Membrane charge moved at contraction thresholds in skeletal muscle fibers. *Journal of Physiology*. 314:595–633.
- Huang, C. L.-H. 1981. Dielectric components of charge movements in skeletal muscle. *Journal of Physiology*. 313:187–205.
- Huang, C. L.-H. 1982. Pharmacological separation of charge movement components in frog muscle. *Journal of Physiology*. 324:375–387.
- Hui, C. S. 1983. Pharmacological studies of charge movement in frog skeletal muscle. *Journal of Physiology*. 337:509–529.
- Kovács, L., E. Rios, and M. F. Schneider. 1979. Calcium transients and intramembrane charge movement in skeletal muscle fibers. *Nature*. 279:391–396.
- Kovács, L., and M. F. Schneider. 1978. Contractile activation by voltage clamp depolarization of cut skeletal muscle fibres. *Journal of Physiology*. 277:483–506.
- Kovács, L., and G. Szücs. 1983. Effect of caffeine on intramembrane charge movement and calcium transients in cut skeletal muscle fibers of the frog. *Journal of Physiology*. 341:559–578.
- Melzer, W., M. F. Schneider, B. J. Simon, and G. Szücs. 1986. Intramembrane charge movement and calcium release in frog skeletal muscle. *Journal of Physiology*. 373:481–511.

- Palade, P. T., and R. L. Barchi. 1977. On the inhibition of muscle membrane chloride conductance by aromatic carboxylic acids. *Journal of General Physiology*. 69:879–896.
- Rakowski, R. F. 1981. Immobilization of membrane charge in frog skeletal muscle by prolonged depolarization. *Journal of Physiology*. 317:129–148.
- Rakowski, R. F., P. M. Best, and M. R. James-Kracke. 1985. Voltage dependence of membrane charge movement and calcium release in frog muscle fibres. *Journal of Muscle Research and Cell Motility*. 6:403–433.
- Rios, E., and G. Brum. 1987. Involvement of dihydropyridine receptors in excitation-contraction coupling in skeletal muscle. *Nature*. 325:717–720.
- Scarborough, J. B. 1966. Numerical Mathematical Analysis. The John Hopkins Press, Baltimore, MD. 545–547.
- Schneider, M. F., and W. K. Chandler. 1973. Voltage dependent charge movement in skeletal muscle: a possible step in excitation-contraction coupling. *Nature*. 242:244–246.
- Schneider, M. F., and W. K. Chandler. 1976. Effects of membrane potential on the capacitance of skeletal muscle fibres. *Journal of General Physiology*. 67:125–163.
- Simon, B. J., and K. G. Beam. 1985. The influence of transverse tubular delays on the kinetics of charge movement in mammalian skeletal muscle. *Journal of General Physiology*. 85:21–42.
- Tsien, R. W., and D. Noble. 1969. A transition state theory approach to the kinetics of conductance changes in excitable membranes. *Journal of Membrane Biology*. 1:248–273.
- Woll, K. H., M. D. Leibowitz, B. Neumke, and B. Hille. 1987. A high-conductance anion channel in adult amphibian skeletal muscle. *Pflügers Archiv*. 410:632–640.